RSO Simulations with Anti-Sun Pointing Predictions

Randa Qashoa
York University
Regina S.K. Lee
York University
Ryan Clark
C-CORE

ABSTRACT

A major component of Space Situational Awareness (SSA) is the ability to predict, track and identify Resident Space Objects (RSO) in orbit. High fidelity RSO simulators are a critical tool in developing RSO tracking and detecting algorithms to generate simulated star field images with accurate representation of RSOs. RSO characteristics such as position, velocity, etc. are calculated from Two-Line Element (TLE), Orbital Mean-Elements Message (OMM), or ephemeris data. Most RSO simulators used in today's SSA studies (including [1], developed in our research team) lack pre-built attitude profiles of the host observer, which is needed to determine the sensor's boresight, or pointing direction. In this study, we present improvements to the simulator to include a wider range of inputs for the attitude information. Specifically, by introducing a known pointing profile for the satellite we can make more accurate predictions of the RSO's position and velocity.

In exploring the addition of a known pointing profile to the simulator in cases where attitude information is lacking, we additionally limit ourselves to low-resolution cameras, akin to the ones used in star trackers, although the simulator can support high-resolution image generation as well. We limit the study to low-resolution imagers because high resolution imagers typically have known attitude information. Images from Cascade, Smallsat and Ionospheric Polar Explorer's (CASSIOPE's) Fast Auroral Imager (FAI) sensor were chosen due to similar sensor parameters to star trackers and the availability of public ephemeris files that we can use to generate even more realistic simulations for comparison. With the ephemeris and attitude information it is possible to extract the exact boresight vector for the sensor for every timestamp being studied. The FAI is currently locked in an anti-sun pointing mode due to a recent issue with CASSIOPE's reaction wheels [2] making it an ideal candidate for this study. An anti-sun pointing mode was implemented within the simulator and simulated images from ephemeris files will be used as validation data.

The validation will be accomplished by simulating FAI images that were predicted using the anti-sun pointing mode with simulated images generated using true ephemeris files that contain attitude information. In comparing the images, we will look at specific targets' temporal features. Some of the temporal features we will compare are the entry and exit times between both sets of images as well as the observation duration between both methods. By proving the ability to predict a certain, known, spacecraft orientation with the simulator, we can then further improve its prediction capabilities by adding more orientation modes.

Many satellites utilize specific orientation profiles to achieve their various mission goals. Such pointing modes include anti-sun, nadir, or inertial pointing. Most satellites have known pointing modes which they reside in most of the time. However, they do not have publicly available attitude information, which impacts our ability to simulate images of star fields and RSOs. Our proposed solution is to use the pointing modes to approximate the attitude of the spacecraft so we can generate more accurate simulated images in cases where we are limited by the insufficient amount of data.

1. INTRODUCTION

An important part of Space Situational Awareness (SSA) and mitigating the concern of the increase in the number of Resident Space Objects (RSOs) is to detect and track the RSOs with accurate orbit and attitude information of the objects. This tool helps address the concern for the proliferation of RSOs which inevitably increases the risk of collisions for satellites. Thus, to provide timely and accurate information to enable safe and sustainable space operations, the tracking and identification of RSOs is of the utmost importance [3]. There are many ways to accomplish the tracking and identification of RSOs. One of which is by taking images of star fields and identifying RSOs within them and looking at the positions of the various objects over multiple frames of an image sequence. Using this information and the time at which the object leaves the observer's field of view, one can correlate the object to a North American Aerospace Defense Command (NORAD) catalog number and/or determine some astrometric properties. However, in order to develop and test such algorithms, many validation images with known target RSOs are needed, but are scarcely publicly available with labeled data sets.

In order to develop algorithms for RSO detection and tracking, often large datasets (labeled and annotated with orbit and attitude information) are required for training and accuracy validation. This is especially the case if we need to develop Machine Learning (ML) algorithms as they require millions and sometimes even billions of inputs in a dataset for training. Given the difficulty of obtaining such large quantities of data needed for training such algorithms, image simulations can be used for algorithm training. Simulations can easily be used to generate large quantities of labeled data with a lot of options for obtaining a variety of data by modifying one or more parameters within these simulators. Lack of labeled data is of the greatest challenge as in many applications and RSO images are no exception. There is no publicly available annotated data that can be easily used for algorithm design. Furthermore, manual labeling is extremely difficult given the nature of these images. For example, medical images are considered difficult because of the need for experts to label them. Cityscapes are challenging to annotate because of the large amount of subjectivity that could result from placing incorrect bounding boxes (or those of the wrong size) or even missing some labels when some smaller objects are neglected. Similarly, differentiating RSOs from stars and detecting them requires sequences of images instead of a single image, pre-processing to remove a lot of the noise to be able to see the potential RSOs and prior experience to be able to properly label RSOs.

Simulated images are often used in place of labeled real RSO images to provide accurate data. The accuracy of these images is critical for the development of analytical algorithms as we have truth data on the RSO and is helpful for training ML algorithms that perform well. Using simulated data to train ML algorithms is not an uncommon practice in this challenging field. For example, in [4], simulated light curves are used to train a ML algorithm for RSO light curve classification and in [5], simulated RSO images are used for RSO streak detection. By increasing the accuracy of RSO and star-field image simulators, we ease the process of transitioning from a fully simulated dataset to testing on real datasets.

We have developed a star-field image simulator in [1] to help address the need for simulated datasets. The observer's position, velocity, and attitude can be determined by supplying an ephemeris file containing these measured values or by using a TLE file. For the purpose of generating realistic and accurate images, ephemeris files are preferred as they provide true values at almost constant instances (typically 1 second apart) as opposed to TLEs which must be propagated to the time of interest. One way to use TLEs when attitude files are unavailable is by specifying the orientation profile of the RSO as TLEs store information regarding the orbit of the RSO which can be used to extract position and velocity with no way to determine attitude. The only other method of using TLEs when attitude is unavailable is to generate tracking mode images where the sensor tracks a specified target such that it is always in the center of the image. By providing rough estimates of the RSO's attitude profile, we can obtain simulated images in cases that were not possible before. Many RSOs have typical pointing modes to accomplish different objectives such as anti-sun pointing, nadir, or inertial pointing. By implementing such attitude modes within the pre-existing RSO simulator, we can improve the fidelity even when we do not have detailed attitude files. In this paper, we present the implementation of anti-sun pointing mode to accompany TLEs for RSO simulations when detailed attitude information is unavailable. The results presented are those with pointing mode operation of the Cascade, Smallsat and Ionospheric Polar Explorer (CASSIOPE) satellite particularly the Fast Auroral Imager (FAI) that is currently locked in a roughly anti-sun pointing mode. CASSIOPE has publicly available ephemeris data which will be used to test the results obtained by using a combination of TLEs and anti-sun pointing mode.

In Section 2, we describe the RSO simulator and CASSIOPE in more detail. In Section 3, the simulation sequences are discussed, followed by methodology of implementing anti-sun pointing and the simulation approach in Section 4. The results are shown and discussed in section 5 and the final remarks with the future tasks are provided in Section 6.

2. BACKGROUND

2.1 RSO Simulator

The RSO simulator, referred to as Space-Based Optical Image Simulator (SBIOS) was initially developed during a feasibility study to determine whether star trackers can be used for RSO imaging. FAI simulations from SBOIS have been compared with STK-EOIR and real images in [1]. SBOIS has since been expanded to include many other features such as tracking mode implementation and ground-based imaging. We are continuously looking for methods to improve the simulator and the next step in that is adding attitude modes which we have done for anti-sun pointing in this study. Prior to adding anti-sun pointing, the only other method of performing simulations without ephemeris files required using TLEs with an attitude file containing the values of yaw, pitch, and roll for every second used in the simulator. Obtaining detailed attitude files are just as challenging as obtaining ephemeris files so by estimating the attitude as belonging to a certain profile (which applies to many RSOs), we can perform simulations on objects we were not able to before. By expanding the capability of the RSO simulator to generate images from any observer we were unable to simulate from previously, we added a larger variety of simulated images that can be used for ML training which potentially improves the performance of these algorithms. In [6], for example, simulated images were used for developing a classifier that differentiates stars, RSOs, and noise.

Simulated RSO data are also used in other areas of SSA research beyond AI-based detection algorithm design such as light curve analysis [7]. There have been several studies that proposed designs of RSO simulators such as [8] and [9]. While most simulators are designed to generate data that solve very specific problems within SSA, the RSO simulator used within this study has the potential to be used for a wide variety of applications such as light curve analysis, attitude estimation, and RSO and streak detection. The simulator described in this study is capable of generating space-based images from any existing RSO which is why the lack of attitude information can be a challenge and implementing attitude modes will be an asset to SSA.

2.2 CASSIOPE

CASSIOPE is a Canadian space weather satellite with multiple cameras and sensors. One of the main payloads is the FAI which was designed to study the aurora in the 650-1100 nm wavelength scale [10]. Recently, we have used FAI images to demonstrate that wide filed-of-view (FOV) cameras like star trackers and FAI imagers are capable of imaging RSOs for SSA applications [11]. The camera specifications of FAI are comparable to a star tracker, which was the main focus of SBOIS, in that it has a low resolution of 256x256. The reason for focusing on low resolution and wide FOV cameras such as star trackers for SSA is that we already have a large number of such sensors in orbit accomplishing different tasks. By using these sensors for SSA, we can utilize already existing hardware in space for newfound purposes such as RSO tracking, detection, and identification. One of the main advantages of using CASSIOPE as the observer is that the downlinked data from all sensors are publicly available and are easy to access. This includes FAI images as well as ephemeris files that contain CASSIOPE's position, velocity, and attitude information. This makes CASSIOPE the ideal RSO to use for SSA algorithm development and validation due to the availability of real data. Once the feasibility of a certain technique has been proven using CASSIOPE, the algorithms can be extended for studies on other RSOs.

Prior to 2021, CASSIOPE was able to point at specified targets. Unfortunately, at the end of 2021, CASSIOPE's 3 out of 4 reaction wheels ceased to function so the satellite is no longer able to point at targets [2]. Instead, the spacecraft is oriented such that its top solar panel is always facing the sun. Due to the location of FAI on the satellite bus, which is on the opposite end of the solar panel, it will point in an anti-sun direction which is ideal for RSO viewing.

3. SIMULATION SEQUENCES

CASSIOPE has publicly available ephemeris files that can be downloaded from University of Calgary's Enhanced Polar Outflow Probe (e-POP) website: https://epop-data.phys.ucalgary.ca. Data from the RSO's first moments of operations in 2013 till today are all available. We have simulated over 600 images using anti-sun pointing to test this new feature in the simulator. The comparison study described in this paper is performed on 3 images taken of RSOs in view of FAI on April 16 and April 22, 2023. These particular dates and time windows were chosen due to the availability of ephemeris files and real images on these days. The targets and estimated entry times used for this analysis are represented in Table 1.

Table 1: List of Studied RSOs

Sequence Number	**Estimated Start Time (UTC)**	**Target Name**	**Target NORAD Catalog Number**
1	April 16 15:56:20	USA 40 R/B DEB	23159
2	April 22 05:37:35	OneWeb-0647	56079
3	April 22 23:50:25	Starlink-6101	56115

USA 40 R/B DEB (catalog ID 23159) is a piece of debris from an American rocket body that was launched in 1989 [12]. At the time of observation, this rocket body was approximately 5756 km from CASSIOPE with a phase angle of around 18°.

The target in the second sequence is OneWeb-0647 which is a satellite that was launched on March 26, 2023 [13]. OneWeb satellites have dimensions of 1 m x 1 m x 1.3 m [14]. At the start time of the second sequence, this target was around 1935 km away from CASSIOPE and has a phase angle of about 24.5°.

Lastly, the third sequence targets Starlink-6101 which is another recently launched satellite on March 29, 2023 by SpaceX [15]. At around 23:50:25 UTC, CASSIOPE was able to see Starlink-6101 which was 605 km away with a 16.6° phase angle.

An image of the second target (OneWeb-0647) taken from FAI on April 22nd is shown in Fig. 1a and an image of the third target (Starlink-6101) captured on the same day is illustrated in Fig. 1b. Each of these images has multiple RSOs in view from FAI but, in this analysis, we will only focus on one target per image. The white circle indicates the location of the target RSO. This was determined using the expected location of the RSO from the ephemeris-based simulations.

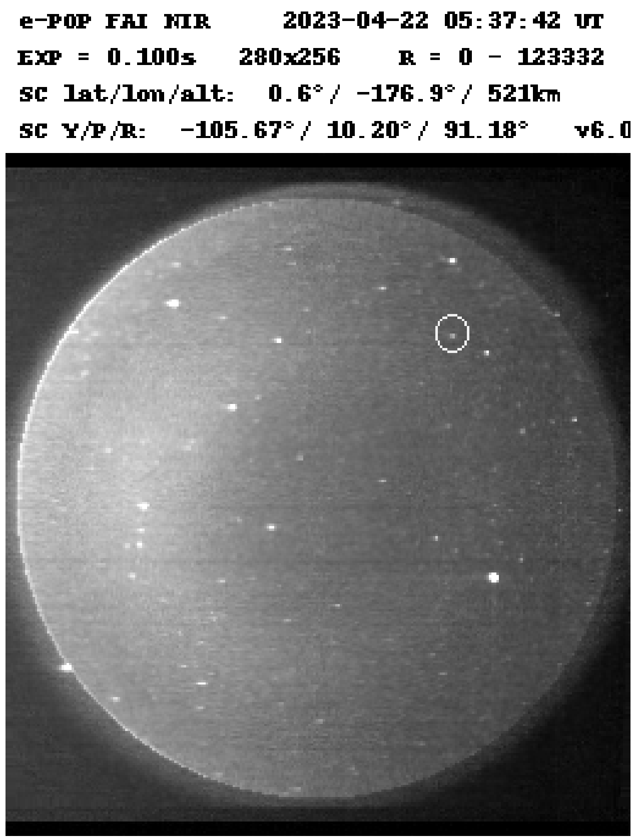

(a) $Target : OneWeb - 0647$

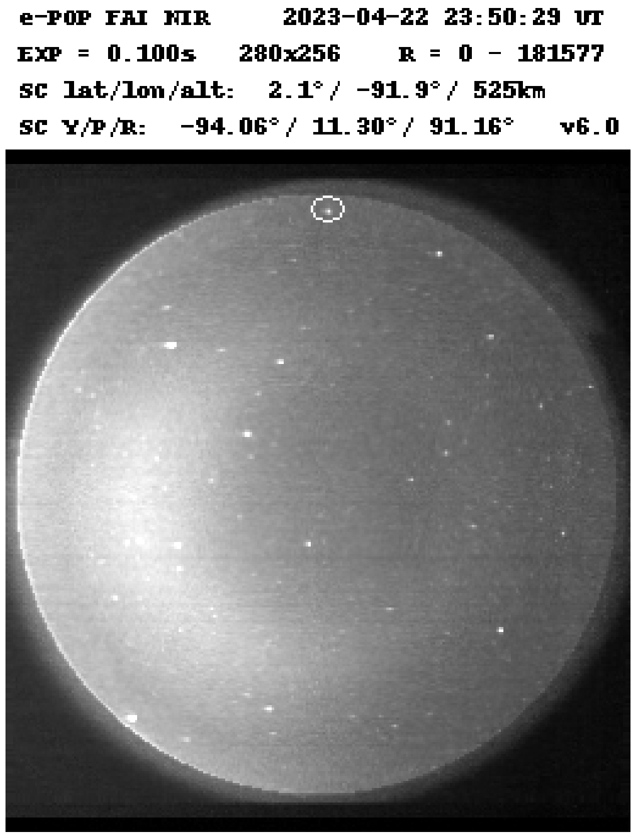

(b) $Target : Starlink - 6101$

Fig. 1: Real FAI images captured on April 22, 2023

In close-up, images of the above targets appear to be 4 and 6 lit pixels, respectively as shown in Fig. 2.

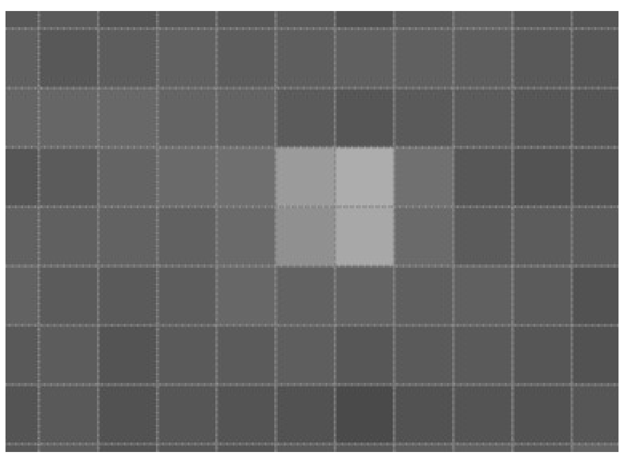

(a) $Target : OneWeb - 0647\,(4\,lit\,pixels)$

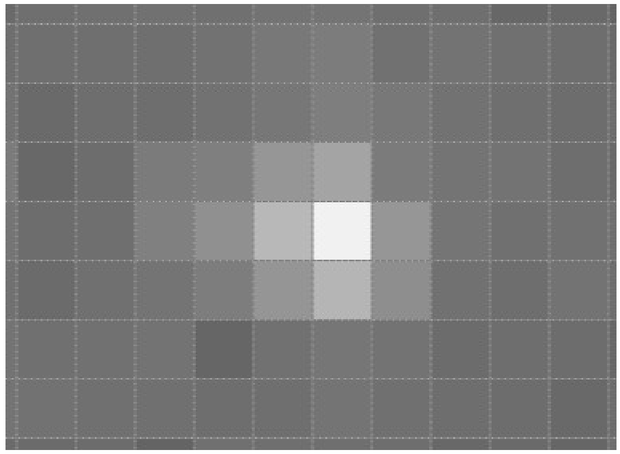

(b) $Target : Starlink - 6101\,(5\,lit\,pixels)$

Fig. 2: Lit Pixels of Targets from Real FAI Images

4. METHODOLOGY

4.1 Anti-Sun Pointing

In order to orient the RSO in an anti-sun pointing direction, we need to first obtain the sun's position in the Earth Centered Inertial (ECI) frame. Then, we invert the sun's ECI coordinates to point anti-sun and convert to the host satellite's, which is FAI in this case, orbital frame. With the RSO in the orbital frame, we can convert the RSO's position vector to obtain the attitude needed to point to that vector, which is anti-sun in this case. To perform this conversion, we need the RSO's position in both the orbital frame as well as the body frame which we are assuming to be fixed on the z-axis. Using these two vectors, we need to calculate two matrices, which will be referred to as G and F for this study, and find the rotation matrix between them. The expression for G is shown in equation 1.

$$G = \begin{bmatrix} \mathbf{RSO_{Orb}} \cdot \mathbf{RSO_{Body}} & -norm(\mathbf{RSO_{Orb}}) \times \mathbf{RSO_{Body}}) & 0 \\ norm(\mathbf{RSO_{Orb}} \times \mathbf{RSO_{Body}}) & \mathbf{RSO_{Orb}} \cdot \mathbf{RSO_{Body}} & 0 \\ 0 & 0 & 1 \end{bmatrix} \tag{1}$$

The expression for the F matrix is in equation 2.

$$F = \begin{bmatrix} \mathbf{RSO_{Orb}} \\ \\ \dfrac{\mathbf{RSO_{Body}} - (\mathbf{RSO_{Orb}} \cdot \mathbf{RSO_{Body}}) * \mathbf{RSO_{Orb}}}{(\mathbf{RSOBody} - norm(\mathbf{RSO_{Orb}} \cdot \mathbf{RSO_{Body}} * \mathbf{RSO_{Orb}}} \\ \mathbf{RSO_{Body}} \times \mathbf{RSO_{Orb}} \end{bmatrix}^{\mathrm{T}} \tag{2}$$

Using both the G and F matrices, the rotation matrix can be calculated using equation 3.

$$RSO_{rotation} = (FGF^{-1})^{\mathrm{T}} \tag{3}$$

With the rotation matrix, we can calculate the yaw, pitch, and roll as shown in equations 4 - 6.

$$Yaw = \tan^{-1}\left(\frac{RSO_{rotation}(2,1)}{RSO_{rotation}(1,1)}\right) \tag{4}$$

$$Pitch = \tan^{-1}\left(\frac{-RSO_{rotation}(3,1)}{\sqrt{RSO_{rotation}(3,2)^2 + RSO_{rotation}(3,3)^2}}\right) \tag{5}$$

$$Roll = \tan^{-1}\left(\frac{RSO_{rotation}(3,2)}{RSO_{rotation}(3,3)}\right) \quad (6)$$

A summary of the steps needed to determine the attitude of the RSO in anti-sun pointing is described in Fig: 3

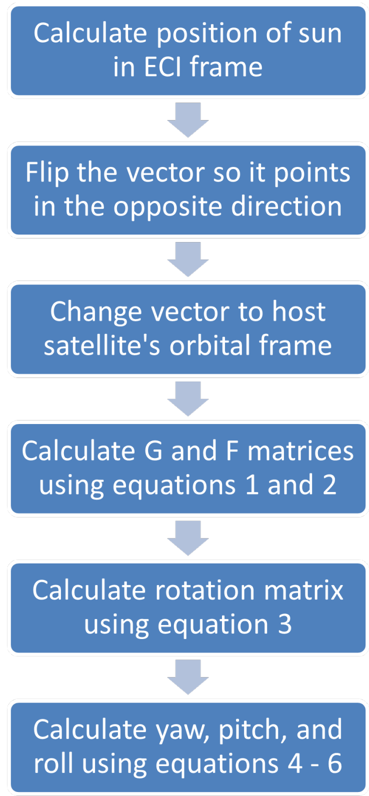

Fig. 3: Flowchart for determining anti-sun pointing attitude

For each time stamp, the simulator outputs an image as well as a data file containing information on the observed targets including their NORAD catalog number, distance to the host, and position in ECI.

4.2 Comparison Approach

For this study, we have decided to perform a temporal comparison between simulated images generated using ephemeris files, which are essentially truth data, as well as simulated images generated using TLEs in anti-sun pointing mode. We compared the time of entry and exit between the two approaches as well as the observation duration.

5. RESULTS AND DISCUSSION

We generated simulated images of FAI using anti-sun pointing mode and with ephemeris files. To ensure we captured the full entry and exit times of all target RSOs, we generated simulations with a 2-minute buffer from the start times listed in Table 1. A sample simulated image from sequence 3 is depicted in Fig. 4. The artifact on the left of Fig. 4b is the Earth's limb. There is a slight difference in the boresight right ascension and declination such that the Earth limb does not appear in Fig. 4a.

Using the resulting data file that includes the information of the observed targets, we extracted the entry and exit times for each target. The results from the ephemeris file simulation are summarized in Table 2.

The next step in the study was to generate the same sequences but using CASSIOPE's TLE with anti-sun pointing instead of its ephemeris files. The results are summarized in Table 3.

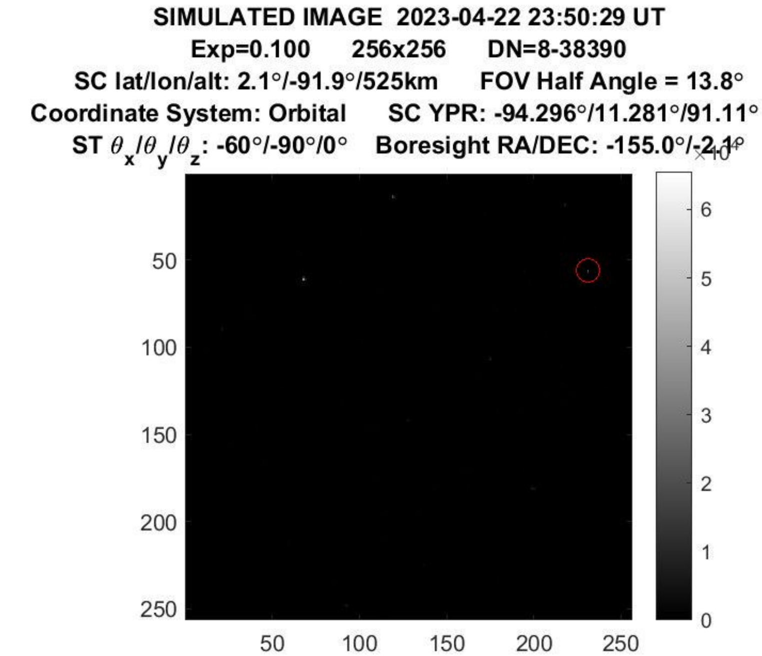

(a) *Generated Using Ephemeris File*

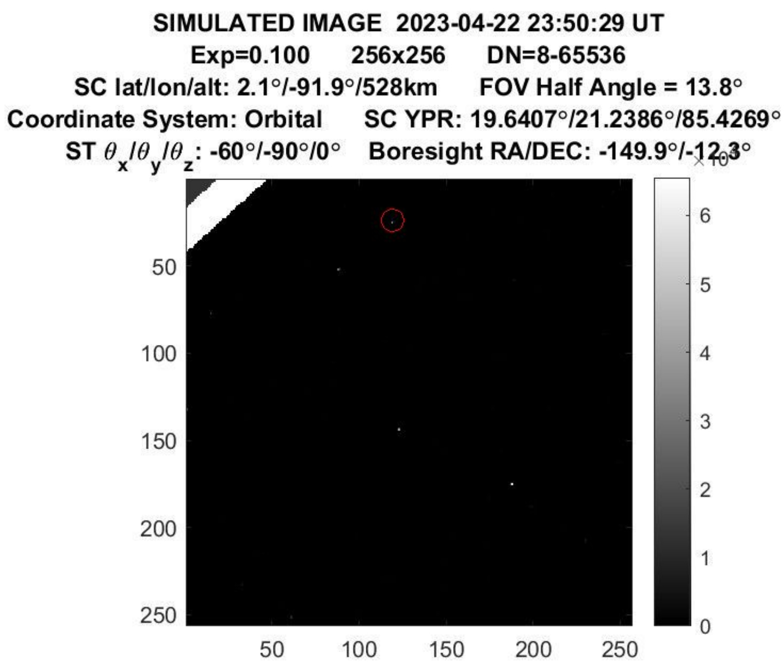

(b) *Generated Using Anti − Sun Pointing Profile*

Fig. 4: Simulated Images Generated Using 2 Methods on April 15, 2023, 00:30:31 UTC

By subtracting the value of start time and end time between the two methods, we obtain Table 4. Negative values indicate that anti-sun pointing simulations start or end earlier, or are shorter than ephemeris file simulations.

Table 2: Ephemeris File Sequence Entry and Exit Times

Sequence Number	Catalog Number	Start Time (UTC)	End Time (UTC)	Duration (Seconds)
1	23159	15:56:21	15:58:01	100
2	56079	05:37:37	05:38:00	23
3	56115	23:50:27	23:50:33	6

Table 3: Anti-Sun Pointing Sequence Entry and Exit Times

Sequence Number	Target Catalog Number	Start Time (UTC)	End Time (UTC)	Duration (Seconds)
1	23159	15:55:00	15:57:35	155
2	56079	05:37:01	05:38:10	69
3	56115	23:50:18	23:50:35	17

Table 4: Difference Between Anti-Sun Pointing and Ephemeris File Sequence Entry and Exit Times in Seconds

Sequence Number	Target Catalog Number	Start Time Difference	End Time Difference	Duration Difference
1	23159	-81	-26	55
2	56079	-36	10	46
3	56115	-9	-2	11

By comparing the two tables, we can notice that the same targets are still visible when using TLEs and anti-sun pointing mode but there is a difference in the entry and exit times compared to using ephemeris files only. The largest difference is 81 seconds which indicates that anti-sun pointing is still a viable method when ephemeris files are unavailable. In these examples, using anti-sun pointing mode, we can have earlier predictions of when a target RSO would be in view but the there is no specific trend on whether anti-sun pointing estimation predicts RSOs exiting earlier or later than when using ephemeris files. The fact that the same target RSO is in view of the sensor using such a prediction within a minute and a half accuracy proves the viability of using such predictions when detailed attitude information is unavailable.

6. CONCLUSION

In conclusion, an improved simulator with the anti-sun pointing mode feature has been developed to perform simulations when detailed attitude information is not available, and the observer is known to be pointing in an anti-sun direction. This allows us to expand the number of simulated RSOs as ephemeris files are rarely made public and there is no other method of generating stare-mode simulated images. At all 3 sequences, we were able to see the specified targets with a maximum difference in entry and exit time of 81 seconds. The maximum difference occurs in the longest sequence and the difference drops down with shorter sequences. For a long sequence, the difference in entry time is less than 2 minutes so for estimates when ephemeris files are unavailable, we can use pre-built attitude profiles. The results presented here are of a limited initial test and we will find and test new sequences with anti-sun pointing simulations, ephemeris file simulations, and real images. The results in this paper are significant as we are able to accurately replicate images for mission planning and ML algorithm training for a wider variety of RSOs with the added attitude profiles.

Future work includes adding additional attitude profiles within the simulator, such as nadir or inertial pointing. Other areas of improvement within the simulator that are currently under development include: illumination conditions, facet model update, light curve models, and much more.

7. REFERENCES

[1] Ryan Clark, Yanchun Fu, Siddharth Dave, and Regina Lee. Simulation of RSO images for space situation awareness (ssa) using parallel processing. *Sensors*, 21, 2021. https://doi.org/10.3390/s21237868 doi:10.3390/s21237868.

[2] Routine CASSIOPE (Swarm-Echo) science operations come to an end – e-POP on CASSIOPE. URL: https://epop.phys.ucalgary.ca/routine-cassiope-swarm-echo-science-operations-come-to-an-end/.

[3] John A Kennewell and Ba-Ngu Vo. An overview of space situational awareness. In *Proceedings of the 16th International Conference on Information Fusion*, pages 1029–1036, July 2013.

[4] Katiyayni Balachandran and Dr. Kamesh Subbarao. Classification of resident space objects by shape and spin motion using neural networks and photometric light curves. 2021. URL: http://conference.sdo.esoc.esa.int,.

[5] Zhe Chen, Yang Yang, Anne Bettens, Youngho Eun, Xiaofeng Wu, and au Xiaofeng Wu. A simulation-augmented benchmarking framework for automatic RSO streak detection in single-frame space images. 4 2023. URL: https://arxiv.org/abs/2305.00412v1.

[6] Siddharth Dave, Ryan Clark, and Regina S.K. Lee. RSOnet: An image-processing framework for a dual-purpose star tracker as an opportunistic space surveillance sensor. *Sensors*, 22, 2022. https://doi.org/10.3390/s22155688 doi:10.3390/s22155688.

[7] M Cegarra, R Abay, S Gehly, A Lambert, P Lorrain, S Balage, M Brown, and C Bright. Attitude detection of Buccaneer RMM cubesat through experimental and simulated light curves in combination with telemetry data. 2018. URL: www.amostech.com.

[8] Wei Zhang, Zhiguo Jiang, Haopeng Zhang, and Jianwei Luo. Optical image simulation system for space surveillance. *Proceedings - 2013 7th International Conference on Image and Graphics, ICIG 2013*, pages 721–726, 2013. https://doi.org/10.1109/ICIG.2013.146 doi:10.1109/ICIG.2013.146.

[9] Susan P. Hagerty and H. Benton Ellis. A high fidelity approach to data simulation for space situational awareness missions. *AMOS Conference*, 2016.

[10] Leroy Cogger, Andrew Howarth, Andrew Yau, Andrew White, Greg Enno, Trond Trondsen, Don Asquin, Blair Gordon, Paul Marchand, Danny Ng, Greg Burley, Marc Lessard, and Brent Sadler. Fast Auroral Imager (FAI) for the e-POP mission, 2015. https://doi.org/10.1007/s11214-014-0107-x doi:10.1007/s11214-014-0107-x.

[11] Samuel Clemens, Regina Lee, Paul Harrison, Magellan Aerospace, and Warren Soh. Feasibility of using commercial star trackers for on-orbit resident space object detection. 2018. URL: www.amostech.com.

[12] N2yo USA 40 R/B DEB. URL: https://www.n2yo.com/satellite/?s=23159.

[13] N2yo OneWeb-0647. URL: https://www.n2yo.com/satellite/?s=56079.

[14] eoPortal OneWeb minisatellite constellation. URL: https://www.eoportal.org/satellite-missions/oneweb#spacecraft.

[15] N2yo Starlink-6101. URL: https://www.n2yo.com/satellite/?s=56115.